molecular pharmaceutics

Article

pubs.acs.org/molecularpharmaceutics

Different Effect of Hydrogelation on Antifouling and Circulation Properties of Dextran–Iron Oxide Nanoparticles

Priya Prakash Karmali,[†] Ying Chao,[‡] Ji-Ho Park,[§] Michael J. Sailor,[∥] Erkki Ruoslahti,[†,⊥] Sadik C. Esener,[#] and Dmitri Simberg*[,‡]

[†]Cancer Research Center, Sanford-Burnham Medical Research Institute, 10901 North Torrey Pines Road, La Jolla, California 92037, United States

[‡]Moores Cancer Center, University of California San Diego, 3855 Health Sciences Drive, La Jolla, California 92093, United States

[§]Department of Bio and Brain Engineering, Korea Advanced Institute of Science and Technology, 291 Daehak-ro, Yuseong-gu, Daejeon 305-701, South Korea

[∥]Department of Chemistry and Biochemistry, University of California San Diego, 9500 Gilman Drive, La Jolla, California 92093, United States

[⊥]Vascular Mapping Center, Sanford-Burnham Medical Research Institute at UCSB, 1105 Life Sciences Technology Building, University of California Santa Barbara, California 93106-9610, United States

[#]Department of Nanoengineering, University of California at San Diego, 9500 Gilman Drive, La Jolla, California 92093, United States

Supporting Information

ABSTRACT: Premature recognition and clearance of nanoparticulate imaging and therapeutic agents by macrophages in the tissues can dramatically reduce both the nanoparticle half-life and delivery to the diseased tissue. Grafting nanoparticles with hydrogels prevents nanoparticulate recognition by liver and spleen macrophages and greatly prolongs circulation times in vivo. Understanding the mechanisms by which hydrogels achieve this "stealth" effect has implications for the design of long-circulating nanoparticles. Thus, the role of plasma protein absorption in the hydrogel effect is not yet understood. Short-circulating dextran-coated iron oxide nanoparticles could be converted into stealth hydrogel nanoparticles by cross-linking with 1-chloro-2,3-epoxypropane. We show that hydrogelation did not affect the size, shape and zeta potential, but completely prevented the recognition and clearance by liver macrophages *in vivo*. Hydrogelation decreased the number of hydroxyl groups on the nanoparticle surface and reduced the binding of the anti-dextran antibody. At the same time, hydrogelation did not reduce the absorption of cationic proteins on the nanoparticle surface. Specifically, there was no effect on the binding of kininogen, histidine-rich glycoprotein, and protamine sulfate to the anionic nanoparticle surface. In addition, hydrogelation did not prevent activation of plasma kallikrein on the metal oxide surface. These data suggest that (a) a stealth hydrogel coating does not mask charge interactions with iron oxide surface and (b) the total blockade of plasma protein absorption is not required for maintaining iron oxide nanoparticles' long-circulating stealth properties. These data illustrate a novel, clinically promising property of long-circulating stealth nanoparticles.

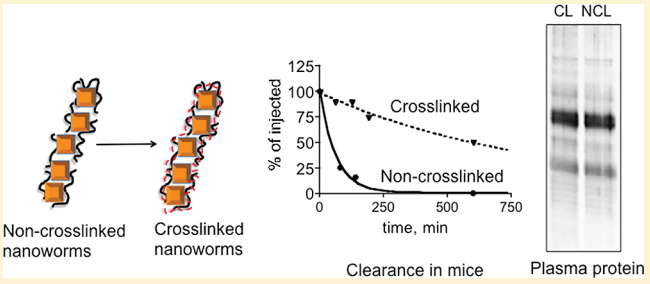

KEYWORDS: *iron oxide, nanoworms, CLIO, SPIO, kininogen, clearance, plasma, stealth, liver*

INTRODUCTION

Sequestration of nanoscale drug/gene delivery systems by macrophages is one of the most serious limitations of *in vivo* nanomedicine.[1] Multiple defense mechanisms with overlapping specificities efficiently recognize and sequester the injected foreign materials.[2] The ability to control and reduce immune recognition of nanoparticles can have an enormous impact on the provision of nanomedicines by enabling more efficient imaging and therapy. The most common strategy for preventing immune recognition of nanoparticles and prolonging their half-life in circulation is to decorate the surface of the nanoparticles with repelling hydrophilic polymers such as polyethylene or polypropylene oxides. The mechanism of the prolonged-circulation effect is not clear, but it is thought to be caused by a nonspecific impermeable barrier that sterically prevents the access of plasma proteins and cell receptors.[3]

Dextran-coated superparamagnetic iron oxide nanoparticles (SPIO) are widely used in the clinic as magnetic resonance imaging (MRI) contrast agents. Following intravenous

Received: July 28, 2011
Revised: December 15, 2011
Accepted: January 15, 2012
Published: January 15, 2012

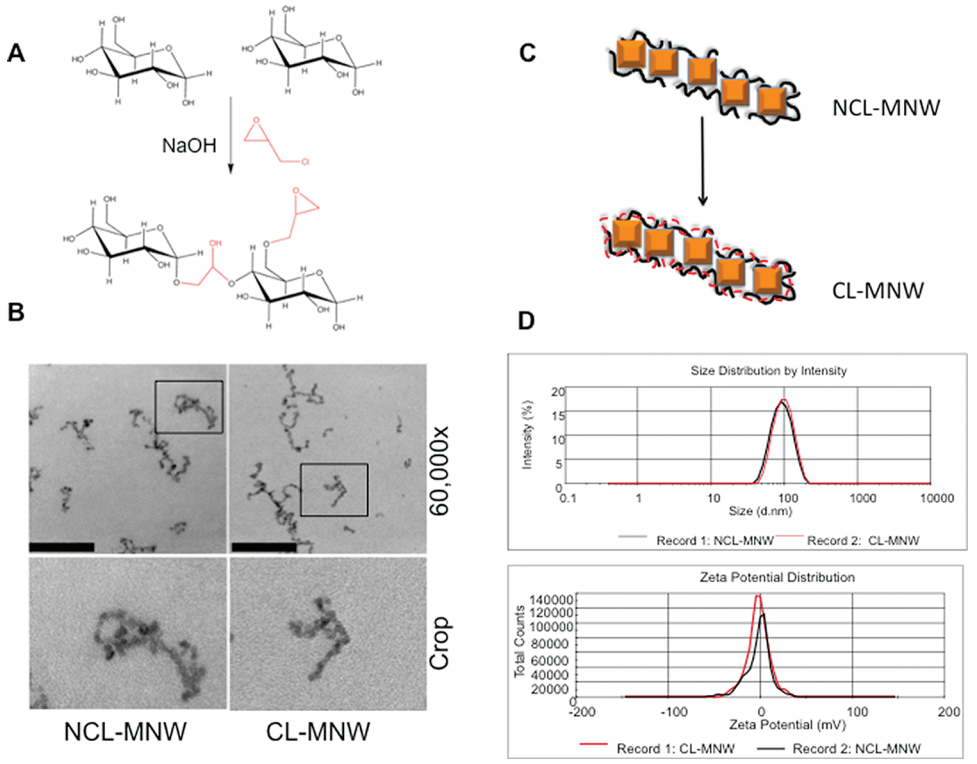

Figure 1. Epichlorohydrin treatment does not affect nanoparticle size, shape, and charge. Magnetic nanoworms (MNW) were converted into cross-linked hydrogel with epichlorohydrin and analyzed as described in Materials and Methods. (A) Reaction of epichlorohydrin (red) with glucopyranose residues caused cross-linking and alkylation of sugar hydroxyls. (B) Transmission electron microscopy images of MNW with (CL) or without (NCL) epichlorohydrin modification. Lower images are cropped areas in the upper micrographs. Size bar, 100 nm. (C) A schematic representation of the particles before and after hydrogelation. Brown squares are Fe_3O_4 crystals. (D) Size (upper chart) and zeta potential (lower chart) measurements of the nanoparticles before and after hydrogelation.

injection, 50−150 nm SPIO become extensively coated by plasma proteins and are cleared from systemic circulation by resident macrophages in the liver, spleen, and lymph nodes, with a half-life of 1−3 h in humans.[4−6] The structural, physical, and surface properties of iron oxides are well-studied.[7,8] Typical SPIO consist of Fe_3O_4 crystals of ∼5 nm size embedded in a meshwork of branched dextran (10−40 kDa). Fe_3O_4 crystals are slightly anionic due to the partial dissociation of $Fe(OH)_3$.[9,10] Using a high-resolution differential proteomic approach, we previously identified plasma proteins that bind to SPIO.[5] Cationic plasma proteins including high molecular weight kininogen (HMWK) and histidine-proline rich glycoprotein (HPRG) bind to the particles due to the anionic component of the nanoparticles, while immunoglobulins and lectins likely bind to dextran's resultant sugar residues.[11−13]

Recently, cross-linked dextran iron oxide nanoparticles (CLIO) have been described.[14] These nanoparticles are prepared by reacting SPIO with 1-chloro-2, 3-epoxypropane (epichlorohydrin). The alkylating-cross-linking properties of epichlorohydrin result in the formation of a hydrated hydrogel coat.[15,16] Recently, we described the synthesis and targeting properties of elongated CLIO nanoparticles, dubbed magnetic nanoworms (MNW).[17,18] Magnetic nanoworms exhibit long-circulating properties in vivo (up to a 12 h half-life in mice).[18] The cross-linked dextran forms highly hydrated hydrogel.[16,19] By analogy with PEGylated coatings, one could assume that the dextran hydrogel forms a steric barrier that prevents protein absorption of plasma proteins.[3] Here, we studied the effect of dextran cross-linking and hydrogelation on MNW recognition by plasma proteins. Our study reveals unexpected mechanisms related to nonfouling and bioinert properties of long-circulating nanoparticles, and provides important pointers for the future design and fabrication of stealth nanomedicines.

RESULTS

First, we studied the effects of cross-linking on the physicochemical properties of nanoparticles. Hereafter we abbreviate cross-linked magnetic nanoworms as CL-MNW and non-cross-linked ones as NCL-MNW. We prepared NCL-MNW by precipitating 20 kDa dextran with iron salts as described.[20,21] From these nanoparticles, we prepared cross-linked CL-MNW by treatment with 1-chloro-2, 3-epoxypropane (epichlorohydrin)[17] (Figure 1A). Transmission electron microscopy (Figure 1B, Figure S1 in the Supporting Information for low magnification) showed that both NCL-MNW and CL-MNW appeared as wormlike clusters of electron-dense iron oxide crystals, consistent with what has been described previously.[17]

In order to exclude artifacts, we subsequently performed cryo-TEM, which confirmed the wormlike shape (Figure S2 in the Supporting Information). Both TEM and cryo-TEM confirmed that the wormlike shape of nanoparticles is not affected by cross-linking (Figure 1C). Dynamic light scattering measurements (Figure 1D, upper panel) showed that nanoparticle size did not change with the hydrogelation, with initial 96 nm NCL-MNW resulting in 105 nm CL-MNW. The zeta potential values of both types of nanoparticles in water were neutral, with −1.65 mV for SPIO and −2.1 mV for CLIO (Figure 1D, lower panel).

dx.doi.org/10.1021/mp200375x | Mol. Pharmaceutics 2012, 9, 539−545

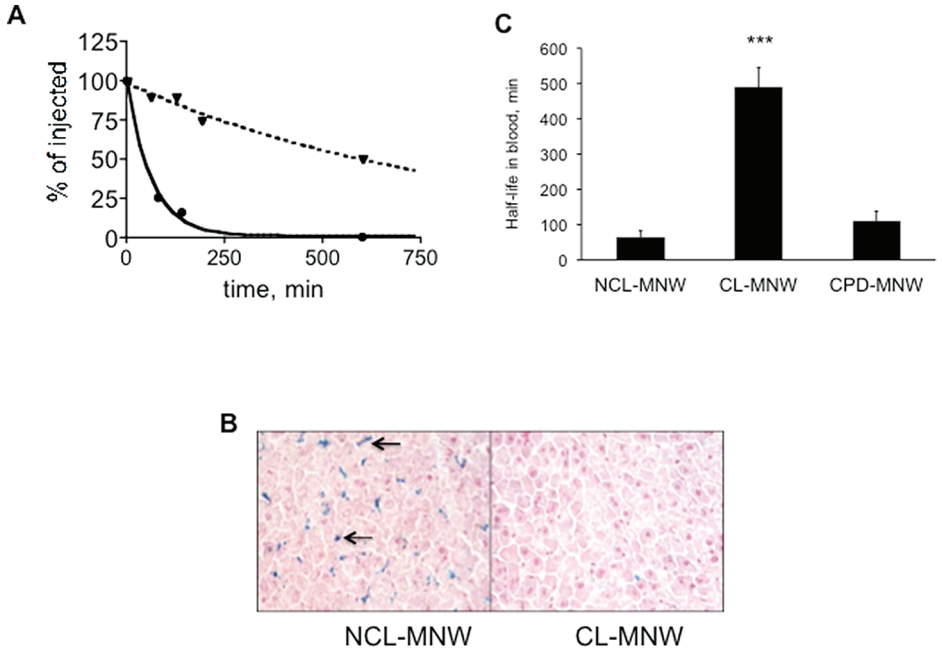

Figure 2. In vivo clearance of nanoparticles is decreased by hydrogelation. Mice were injected with CL-MNW or NCL-MNW (4 mg/kg) and sacrificed by perfusion 4 h postinjection. (A) Concentrations of Fe in plasma were quantified by iron assay and plotted versus time with Prism (GraphPad). CL-MNW (dotted line) and NCL-MNW (solid line) are shown. One representative experiment out of 5 is shown. (C) Histological sections of the livers show almost complete absence of uptake of CL-MNW (right) and strong uptake of CL-MNW (left) by Kupffer cells (arrows) at 4 h postinjection. One representative experiment out of five is shown. (C) MNW half-life shows a 10-fold prolongation after cross-linking with epichlorohydrin. Chloropropanediol-treated nanoworms (CPD-MNW) did not show long-circulating properties, suggesting that alkylation of sugar hydroxyls is not sufficient and that the cross-linking function is required to attain the long-circulating effect. (CPD is a hydrated version of epichlorohydrin and, therefore, lacks the cross-linking action.) p-Value < 0.0001; n = 5 for epichlorohydrin-treated MNW, n = 3 for chloropropanediol-treated MNW (CPD-MNW).

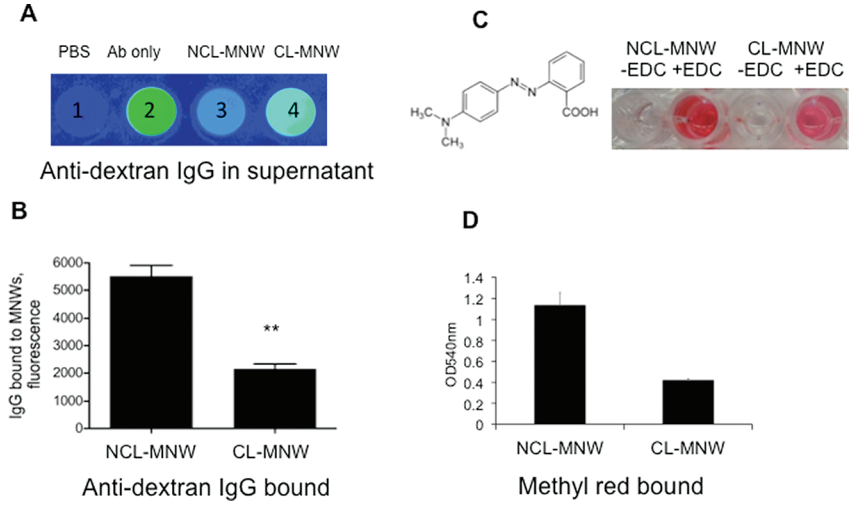

Figure 3. Hydrogelation partially destroys the dextran structure. (A) FITC-labeled anti-dextran antibody was incubated with CL-MNW, with NCL-MNW, or without nanoparticles as described in Materials and Methods. The particles were pelleted down at 100000*g*, and the fluorescence of the supernatant was measured. Anti-dextran IgG binding was calculated by subtracting the fluorescence of wells 3 and 4 from that of well 2. (B) Quantification of anti-dextran IgG binding. CL-MNW bound less of the anti-dextran antibody than the NCL-MNW. p-Value 0.008 (n = 3). (C) The surface hydroxyl groups of MNWs were reacted with methyl red as described in Materials and Methods. Methyl red (structure shown) reacts through its carboxyl group with the hydroxyls in the presence of EDC/NHS. No conjugation to the dextran occurred without EDC. (D) There was about 2 times more methyl red conjugated to NCL-MNW than to CL-MNW, presumably because some hydroxyl groups were consumed during the cross-linking process (n = 2).

In order to determine the effect of cross-linking on nanoparticle circulation in vivo, both CL-MNW and NCL-MNWs were injected into mice. CL-MNW demonstrated around 10-fold prolongation of half-life *in vivo* compared to NCL-MNW (Figure 2A,B). The prolonged clearance of CL-MNW correlated well with these particles' reduced uptake by Kupffer macrophages in the liver (Figure 2B). The methylating and cross-linking effect of epichlorohydrin was required in order to attain these long-circulating properties. When NCL-MNW were treated with 1-chloropropane 2,3-diol (resulting in

dx.doi.org/10.1021/mp200375x | *Mol. Pharmaceutics* 2012, 9, 539–545

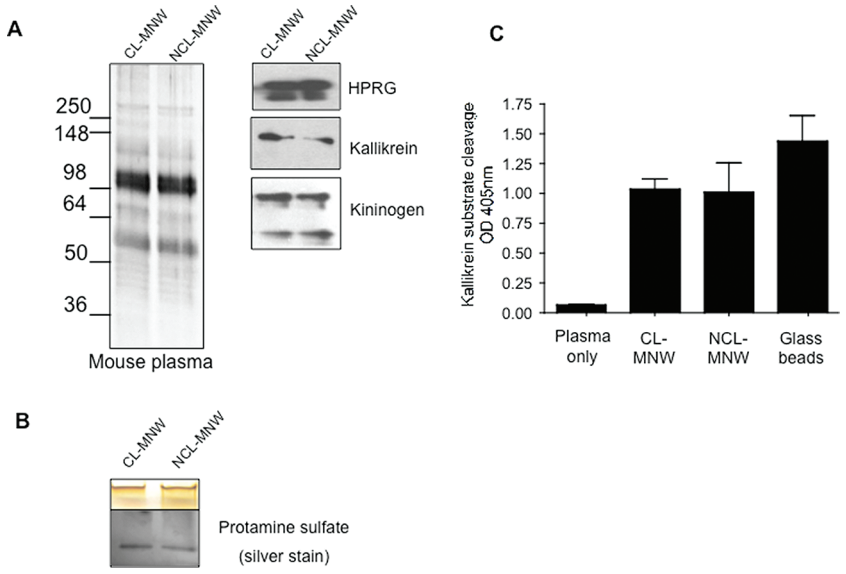

Figure 4. Hydrogelation does not prevent absorption of iron oxide-binding proteins. CL-MNW and NCL-MNW were incubated with citrated mouse plasma or with protamine sulfate as described in Materials and Methods. (A) The nanoparticles were washed and the proteins were eluted and analyzed by SDS−PAGE and silver staining. High molecular weight kininogen (HMWK), histidine-proline rich glycoprotein (HPRG), and plasma kallikrein further were visualized by immunoblotting with specific antibodies; note the similar amounts of proteins adhering to both types of nanoparticles. (B) Silver staining was used to visualize protamine sulfate eluted from the nanoparticles (also shown are the gel wells loaded with equal amounts of MNW). One representative experiment out of 3 is shown. (C) Activation of kallikrein by particles was studied by measuring plasma serine protease activity as described.[5] Micron-sized glass powder was used as a positive control of kallikrein activity. The same level of activation was observed for CL-MNW and NCL-MNW (n = 3).

CPD-MNW), which has only alkylating but no cross-linking properties, there was no improvement in MNW circulation properties (Figure 2C).

To investigate the effects of dextran cross-linking on nanoparticle surface, particles were probed with fluorescein-labeled anti-dextran IgG prior to and following cross-linking. The presence of dextran-binding antibodies has been previously shown in human plasma.[12] Recognition of CL-MNW by anti-dextran IgG was reduced by 60% compared to NCL-MNW (Figure 3A,B, p-value 0.008), suggesting that some sugar epitopes were destroyed by epichlorohydrin. Epichlorohydrin can cross-link between two adjacent hydroxyl groups, generating one hydroxyl, or it can form epoxy adducts that subsequently hydrolyze to form two hydroxyls (Figure 1B); therefore, a net decrease in surface hydroxyls is expected. We conjugated methyl red dye through a carboxyl group to the hydroxyls of the nanoparticle coating and measured the absorbance of the resulting conjugates. Methyl red conjugation was about 60% lower in CL-MNW than in NCL-MNW (Figure 3C,D), suggesting that cross-linking partially destroyed dextran chemical structure and consumed some of its hydroxyls.

We tested whether the stealth effect of epichlorohydrin is caused by an alteration of the sugar structure and/or by a decrease of surface hydroxyls. Branched 500 kDa dextran was conjugated to the surface of CL-MNW and NCL-MNW. The conjugation of dextran 500 kDa resulted in an increase in the diameter of CL-MNW by ∼55 nm (Figure S3A in the Supporting Information). The circulation half-life of Dex500-conjugated NCL-MNW was prolonged by 100%, and Dex500-conjugated CL-MNW was prolonged by 25% (Figure S3B,C in the Supporting Information), suggesting that intact dextran prevents—rather than promotes—nanoparticle recognition.

In order to test whether MNW cross-linking affects nanoparticulate interaction with total plasma protein, CL-MNW and NCL-MNW were incubated with fresh citrated mouse or human plasma (see Materials and Methods). Since the half-life of NCL-MNW is less than 30 min, the proteins that adhere to nanoparticles within 10−30 min are likely the most relevant for clearance. Following 10 min of incubation with plasma, unbound proteins were completely removed by washing (Figure S4 in the Supporting Information). SDS−PAGE and silver staining of the adhered proteins showed that in these experimental conditions plasma proteins stick to both types of nanoparticles to almost the same extent (Figure 4A). Previously we demonstrated that high molecular weight kininogen (HMWK) and histidine-proline rich glycoprotein (HPRG) adsorb on SPIO[5,22] via the histidine-rich sequences. These sequences are known to bind to the anionic surface and to divalent metals.[23,24] Immunoblotting (Figure 4A for mouse plasma and Figure S4 in the Supporting Information for human plasma) shows that CL-MNW and NCL-MNW absorb HPRG and HMWK at similar rates. Kallikrein, which in plasma exists in a complex with HMWK, bound to both types of particles to the same extent (Figure 4A). In addition to histidine-rich proteins, we used protamine sulfate to probe iron oxide charge. Protamine sulfate is an arginine-rich polypeptide that binds to iron oxide through charge interactions.[24] Protamine sulfate absorbed to both types of particles at the same levels (Figure 4B). The binding of kininogen and kallikrein to the foreign surface induces activation of the kallikrein−kinin cascade,[22] due to the association of HMWK−kallikrein and HMWK−FXII complexes with the foreign surface and the activation of kallikrein by Factor FXII.[25] When incubated with whole citrated human plasma, both NCL-MNW and CL-MNW induced potent activation of plasma kallikrein (Figure 4C).

Soluble globular proteins that have a relatively great freedom of movement could penetrate the hydrogel coat by diffusion through the hydrogel pores. We immobilized plasma HMWK

dx.doi.org/10.1021/mp200375x | Mol. Pharmaceutics 2012, 9, 539−545

and its histidine-rich domain D5 on agarose beads, and tested the binding of the nanoparticles. CL-MNW and NCL-MNW showed the same binding efficiency to the immobilized cationic proteins (Figure 5A,B) suggesting that hydrogel does not prevent interactions of nanoworms with the charged protein surface.

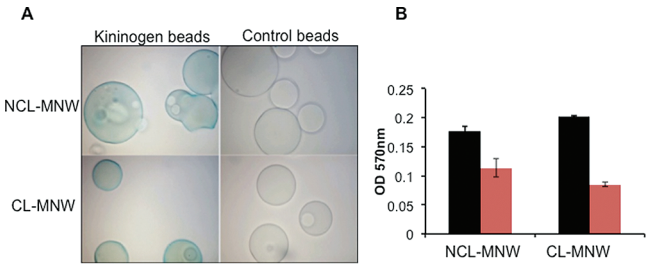

Figure 5. CL-MNW and NCL-MNW bind to cationic protein-coated beads. High molecular weight kininogen or its histidine-rich domain D5 was immobilized onto agarose beads as described in Materials and Methods. (A) HMWK bead-bound iron oxide was visualized with Prussian blue stain, making the beads appear blue. No detectable binding was observed to control antibody-coated beads (for details see Materials and Methods); note the similar levels of binding of CL and NCL MNWs. (B) Quantification of iron oxide binding to HMWK-coated beads (red bars) and to HMWK domain D5-coated beads (black bars) with iron assay. The absorbance of control beads was subtracted. CL-MNWs and NCL-MNWs show similar efficiency of binding to the beads (n = 2 for HMWK beads, n = 4 for D5 beads).

DISCUSSION

It has been previously acknowledged that coating nanoparticles with neutral hydrophilic polymers decreases immune recognition and greatly delays the clearance of many nanoparticulate systems.[26,27] According to Torchilin and Trubetskoy,[28] long chains of polymers such as PEG form a random cloud around the nanoparticle, thereby preventing protein absorption. PEG has been found to prevent binding of plasma proteins.[3] We tested the nonfouling properties of iron oxide nanoworms coated with cross-linked dextran hydrogel in an attempt to explain their long-circulating properties *in vivo*. Our data show that cross-linked dextran hydrogel efficiently prevents MNW recognition and *in vivo* clearance by reticuloendothelial system macrophages, but at the same time allows the binding of numerous plasma proteins and cationic peptides to MNW. A similar phenomenon was observed for PEGylated nanoparticles of certain compositions.[29,30] For example, PEG-DSPE 2000 had no effect on protein adsorption onto negatively charged liposomes composed of phosphatidic acid.[30] It remains to be investigated whether cationic proteins are able to invade and penetrate the hydrogel coating in order to interact with the nanoparticle core, or if there exist some long-range charge interactions on the nanoparticle surface without the hydrogel layer penetration.

Our data show that total repelling of proteins is not required for prolonged circulation of iron oxide nanoparticles. More likely, the prevention of selective interactions is important for attaining these long-circulating properties. Since the molecular pathways responsible for the clearance of nanoparticles are yet to be understood, it would be difficult at this point to suggest a concrete mechanism by which hydrogel prolongs circulation. Particle size and shape play an important role in nanoparticle uptake, possibly due to the decreased ability of macrophages to engulf particles of certain dimensions and shapes.[31−34] However, cross-linking did not significantly affect the size and aspect ratio of our particles. Since the conjugations of intact dextran to CL-MNW surface only further prolonged the clearance of MNWs, we conclude that the cross-linking effect also cannot be ascribed to the alterations of dextran structure. It is likely that there exist subtle differences in protein opsonization that could not be detected in our system. In that case, more sensitive proteomic methods to detect these differences would be required.[5] Other effects, such as the prevention of nanoparticle aggregation *in vivo*, or the inhibition of nanoparticle binding to macrophage surface,[35] are likely to play a role in reducing uptake of the cross-linked nanoparticles. Iron oxide nanoparticles are recognized *in vitro* through scavenger receptor-based mechanisms.[4] As scavenger-receptor signaling and its role in SPIO uptake *in vitro* and *in vivo* become better understood, new clues to nanoparticle biodistribution mechanisms are likely to emerge.

Lastly, the non-bioinert behavior of the hydrogel coatings studied here offers a variety of interesting possibilities for the design of nanoparticles and nanomedicines. There exist potential shortcomings in the nondiscriminating total protein-repelling effect, such as an affinity decrease of surface-tethered ligands due to interference of the surrounding brush PEG layer,[36] and prevention of surface reactions of nanoparticles. Uncoupling of the particles' nonfouling and long-circulating properties could help design smart "semi-stealth" nanomedicines with a broad spectrum of attractive biochemical properties.

MATERIALS AND METHODS

Nanoparticle Preparation and Characterization. Superparamagnetic dextran iron oxide nanoworms were prepared by a precipitation method using 20 kDa dextran (Sigma-Aldrich, St. Louis, MO) as described.[17] For preparation of cross-linked nanoworms (described in detail in ref 17), 15 mg of Fe was reacted in 5 mL of strong base (5 N aqueous NaOH solution) containing 1 mL of epichlorohydrin (Sigma) for 24 h, purified by dialysis against double distilled water for 24 h using a dialysis cassette (10 kDa MWCO, Pierce), and filtered through a 0.1 μm PVDF membrane filter (Millipore, Billerica, MA). The exact same procedure was performed to prepare 1-chloropropane-2,3-diol-treated MNW (Sigma). All particles were stored in PBS at 4 °C prior to use.

Size and ζ (zeta)-potential of nanoparticles before and after dextran modification were measured using Zetasizer Nano (Malvern, U.K.). For nanoparticle imaging with transmission electron microscope, 25 μL of 0.1 mg/mL Fe solution in water was placed on Formvar-/carbon-coated grids (Ted Pella, Redding, CA). After 1 min the grid was gently blotted and air-dried. Grids were viewed using a JEOL 1200EX II (JEOL, Peabody, MA) transmission electron microscope and photographed using a Gatan digital camera (Gatan, Pleasanton, CA).

Clearance and Liver Uptake in Mice. All the animal work was reviewed and approved by the Sanford-Burnham Medical Research Institute's Animal Research Committee. Six- to eight-week old female C57BL/6J mice were anesthetized with Avertin, and nanoparticles (1−4 mg Fe/kg body weight) were injected into the tail vein in a total volume of up to 150 μL. Blood was collected from the periorbital vein by heparinized capillaries at different time points, and plasma was separated from cells by centrifugation using a tabletop microcentrifuge at

4000 rpm for 2 min. Fifteen microliters of plasma was collected to measure iron levels by QuantiChrom Assay (BioAssay Systems, Hayward, CA) as described,[5] and the elimination half-life was determined by Prism (GraphPad, La Jolla, CA) software by plotting the percentage of the injected dose in blood versus time.

For histological analysis of nanoparticle uptake, animals were sacrificed 4 h postinjection, and liver and spleen organs were dissected, fixed in formalin, and cryosectioned; organs were subsequently stained for nanoparticle accumulation using Prussian blue stain and counterstained with Nuclear fast red.

Surface Dextran Probing. Dextran antibody-binding experiments were performed as described previously.[5] Briefly, 3 μL of fluorescein-labeled anti-dextran IgG (STEMCELL Technologies Inc., Vancouver, Canada) were incubated with 100 μg of Fe for 10−15 min. The particles were pelleted by ultracentrifuge, and the FITC fluorescence in the supernatant was measured using a Fuji FLA-5100 fluorescent scanner. The fluorescence associated with nanoparticles, which corresponds to the bound antibody, was calculated as the difference in supernatant fluorescence intensity between antibody and nanoparticle supernatants. For analysis of the dextran hydroxyl groups, a modified methyl red assay was used.[37] Nanoparticles to be analyzed were precipitated in acetone and resuspended in anhydrous DMSO at 2 mg Fe/mL. A 10 mg 1-ethyl-3-[3-dimethylaminopropyl]carbodiimide hydrochloride (EDC, Thermo Fisher Scientific, Waltham, MA), 5 mg methyl red (MP Biomedicals, Solon, OH), 15 mg *N*-hydroxysuccinimide, and 100 μL triethylamine (Sigma-Aldrich) solution was dissolved in DMSO and added to 0.5 mL of 1 mg/mL nanoparticle solution. The reaction was allowed to proceed for 5 h at 37 °C. Thereafter, nanoparticles were precipitated with acetone and resuspended in water five times in order to discard the unreacted methyl red; nanoparticles were subsequently resuspended in 0.3 mL of DDW. Fifty microliters of 10 N HCl was added, and the particles were incubated overnight. This treatment completely dissolved iron oxide, which could otherwise interfere with methyl red absorbance. The absorbance was determined at 540 nm using a Tecan plate reader.

Protein Binding to Nanoparticles. The binding was performed as described.[5] Briefly, 100 μg of iron oxide nanoparticles were incubated with 300−500 μL of fresh citrated mouse or human plasma supplemented with 10 μL of mammalian protease inhibitor cocktail (Sigma), or with 100 μL of 10 mg/mL salmon sperm protamine (Sigma) in PBS, for 10 min with vortexing at room temperature. The unbound proteins were washed away 4 times using a Beckman TLA-100 ultracentrifuge (70000*g* for 10 min in 1 mL of PBS), and the pellet was boiled in 50 μL of 8 M urea/1 M NaCl/1 M imidazole for 30 min. The mixture of particles and proteins (corresponding to 5−20 μg of iron) was loaded into wells of Novex 4−20% Tris-glycine polyacrylamide gel (Invitrogen, Carlsbad, CA), and the proteins were electrophoretically separated and stained with SilverQuest kit (Invitrogen).

For immunoblotting analysis of the eluted proteins, polyclonal goat anti-mouse kallikrein (R&D Systems, Minneapolis, MN), polyclonal mouse anti-human HMWK (R&D), and polyclonal rabbit anti-mouse HMWK (provided by the laboratory of Dr. McCrae) were used.

For binding to kininogen beads, anti-human antibody was immobilized on GammaBind beads (GE Healthcare, Piscataway, NJ) according to the manufacturer's instructions. A ratio of 10 μg of Ab to 100 μL of beads was used. Rabbit antibody (Jackson Immuno Research, West Grove, PA) was used for the preparation of control beads. Following incubation with the antibody, the beads were washed 4 times in PBS and blocked with an excess of rabbit IgG for 10 min.

For immobilizing D5-GST to glutathione-agarose, a previously described protocol was used.[5] GST immobilized on agarose was used as a control. For the nanoparticle binding assay, HMWK-beads, D5 beads, and control beads were incubated with a 0.5 mg/mL solution of nanoparticles for 10 min (50 μL of beads with 50 μL of 1 mg/mL Fe) and washed 4 times in 0.1% Tween-20 in PBS. A small aliquot of the beads was stained with Prussian blue[38] to visualize iron. The rest of the beads were mixed with 200 μL of QuantiChrom Assay overnight, and the absorbance of the supernatant was measured at 570 nm.

■ ASSOCIATED CONTENT

Supporting Information

Experimental details and figures depicting TEM and cryo-TEM images, clearance of dextran-conjugated nanoparticles, and interaction of nanoparticles with human plasma proteins. This material is available free of charge via the Internet at http://pubs.acs.org.

■ AUTHOR INFORMATION

Corresponding Author

*UCSD, Moores Cancer Center, La Jolla, CA 92093. Phone: 858-822-4137. Fax: 858-822-4514. E-mail: dsimberg@ucsd.edu.

■ ACKNOWLEDGMENTS

The authors would like to thank Ms. Emily Bass (UCSD) for assisting with manuscript preparation and Dr. Keith McCrae (Cleveland Clinic) for providing D5-GST and the anti-mouse kininogen antibody. This work was supported by NIH NCI Grants 5U54CA119335 (E.R.) and 1R21CA137721-01 (D.S.) and the UCSD Cancer Center Specialized Support Grant P30 CA23100. We would like to acknowledge the use of the UCSD Cryo-Electron Microscopy Facility, which is supported by NIH grants to Dr. Timothy S. Baker and a gift from the Agouron Institute to UCSD.

■ REFERENCES

(1) Moghimi, S. M.; Hunter, A. C.; Murray, J. C. Long-circulating and target-specific nanoparticles: theory to practice. *Pharmacol. Rev.* **2001**, *53* (2), 283−318.

(2) Taylor, P. R.; Martinez-Pomares, L.; Stacey, M.; Lin, H. H.; Brown, G. D.; Gordon, S. Macrophage receptors and immune recognition. *Annu. Rev. Immunol.* **2005**, *23*, 901−44.

(3) Alexis, F.; Pridgen, E.; Molnar, L. K.; Farokhzad, O. C. Factors affecting the clearance and biodistribution of polymeric nanoparticles. *Mol. Pharmaceutics* **2008**, *5* (4), 505−15.

(4) Raynal, I.; Prigent, P.; Peyramaure, S.; Najid, A.; Rebuzzi, C.; Corot, C. Macrophage endocytosis of superparamagnetic iron oxide nanoparticles: mechanisms and comparison of ferumoxides and ferumoxtran-10. *Invest. Radiol.* **2004**, *39* (1), 56−63.

(5) Simberg, D.; Park, J. H.; Karmali, P. P.; Zhang, W. M.; Merkulov, S.; McCrae, K.; Bhatia, S. N.; Sailor, M.; Ruoslahti, E. Differential proteomics analysis of the surface heterogeneity of dextran iron oxide nanoparticles and the implications for their in vivo clearance. *Biomaterials* **2009**, *30* (23−24), 3926−33.

(6) Bulte, J. W.; Kraitchman, D. L. Iron oxide MR contrast agents for molecular and cellular imaging. *NMR Biomed.* **2004**, *17* (7), 484−99.

(7) Jung, C. W.; Jacobs, P. Physical and chemical properties of superparamagnetic iron oxide MR contrast agents: ferumoxides, ferumoxtran, ferumoxsil. *Magn. Reson. Imaging* **1995**, *13* (5), 661−74.
(8) Jung, C. W. Surface properties of superparamagnetic iron oxide MR contrast agents: ferumoxides, ferumoxtran, ferumoxsil. *Magn. Reson. Imaging* **1995**, *13* (5), 675−91.
(9) Lucas, I. T.; Durand-Vidal, S.; Dubois, E.; Chevalet, J.; Turq, P. Surface charge density of maghemite nanoparticles: Role of electrostatics in the proton exchange. *J. Phys. Chem. C* **2007**, *111* (50), 18568−18576.
(10) Simmons, G. W.; Beard, B. C. Characterization of acid-base properties of the hydrated oxides on iron and titanium metal surfaces. *Langmuir* **1987**, *91* (5), 1143−1148.
(11) Fujita, T.; Matsushita, M.; Endo, Y. The lectin-complement pathway--its role in innate immunity and evolution. *Immunol. Rev.* **2004**, *198*, 185−202.
(12) Chacko, B. K.; Appukuttan, P. S. Dextran-binding human plasma antibody recognizes bacterial and yeast antigens and is inhibited by glucose concentrations reached in diabetic sera. *Mol. Immunol.* **2003**, *39* (15), 933−9.
(13) Arima, Y.; Kawagoe, M.; Toda, M.; Iwata, H. Complement activation by polymers carrying hydroxyl groups. *ACS Appl. Mater. Interfaces* **2009**, *1* (10), 2400−7.
(14) Wunderbaldinger, P.; Josephson, L.; Weissleder, R. Crosslinked iron oxides (CLIO): a new platform for the development of targeted MR contrast agents. *Acad. Radiol.* **2002**, *9* (Suppl. 2), S304−6.
(15) Holmberg, L.; Lindberg, B.; Lindqvist, B. The reaction between epichlorohydrin and polysaccharides: Part 1. Syntheses of some model substances with non-cyclic substituents. *Carbohydr. Res.* **1994**, *262* (2), 213−21.
(16) Denizli, B. K.; Can, H. K.; Rzaev, Z. M. O.; Guner, A. Preparation conditions and swelling equilibria of dextran hydrogels prepared by some crosslinking agents. *Polymer* **2004**, *45* (19), 6431−6435.
(17) Park, J. H.; von Maltzahn, G.; Zhang, L.; Schwartz, M. P.; Ruoslahti, E.; Bhatia, S.; Sailor, M. J. Magnetic Iron Oxide Nanoworms for Tumor Targeting and Imaging. *Adv. Mater.* **2008**, *20*, 1630−1635.
(18) Park, J. H.; von Maltzahn, G.; Zhang, L.; Derfus, A. M.; Simberg, D.; Harris, T. J.; Ruoslahti, E.; Bhatia, S. N.; Sailor, M. J. Systematic surface engineering of magnetic nanoworms for in vivo tumor targeting. *Small* **2009**, *5* (6), 694−700.
(19) Sun, G.; Shen, Y.-I; Ho, C. C.; Kusuma, S.; Gerecht, S. Functional groups affect physical and biological properties of dextran-based hydrogels. *J. Biomed. Mater. Res., Part A* **2010**, *93* (3), 1080−90.
(20) Gupta, A. K.; Gupta, M. Synthesis and surface engineering of iron oxide nanoparticles for biomedical applications. *Biomaterials* **2005**, *26* (18), 3995−4021.
(21) Laurent, S.; Forge, D.; Port, M.; Roch, A.; Robic, C.; Vander Elst, L.; Muller, R. N. Magnetic iron oxide nanoparticles: synthesis, stabilization, vectorization, physicochemical characterizations, and biological applications. *Chem. Rev.* **2008**, *108* (6), 2064−110.
(22) Simberg, D.; Zhang, W. M.; Merkulov, S.; McCrae, K.; Park, J. H.; Sailor, M. J.; Ruoslahti, E. Contact activation of kallikrein-kinin system by superparamagnetic iron oxide nanoparticles in vitro and in vivo. *J. Controlled Release* **2009**, *140* (3), 301−5.
(23) Jones, A. L.; Hulett, M. D.; Parish, C. R. Histidine-rich glycoprotein: A novel adaptor protein in plasma that modulates the immune, vascular and coagulation systems. *Immunol. Cell Biol.* **2005**, *83* (2), 106−18.
(24) Arbab, A. S.; Yocum, G. T.; Kalish, H.; Jordan, E. K.; Anderson, S. A.; Khakoo, A. Y.; Read, E. J.; Frank, J. A. Efficient magnetic cell labeling with protamine sulfate complexed to ferumoxides for cellular MRI. *Blood* **2004**, *104* (4), 1217−23.
(25) Colman, R. W.; Schmaier, A. H. Contact system: a vascular biology modulator with anticoagulant, profibrinolytic, antiadhesive, and proinflammatory attributes. *Blood* **1997**, *90* (10), 3819−43.
(26) Owens, D. E. 3rd; Peppas, N. A. Opsonization, biodistribution, and pharmacokinetics of polymeric nanoparticles. *Int. J. Pharm.* **2006**, *307* (1), 93−102.
(27) Gabizon, A.; Shmeeda, H.; Barenholz, Y. Pharmacokinetics of pegylated liposomal Doxorubicin: review of animal and human studies. *Clin. Pharmacokinet.* **2003**, *42* (5), 419−36.
(28) Torchilin, V. P.; Trubetskoi, V. S. Which polymers can make nanoparticulate drug carriers long-circulating? *Adv. Drug Delivery Rev.* **1995**, *16*, 141−155.
(29) Dos Santos, N.; Allen, C.; Doppen, A. M.; Anantha, M.; Cox, K. A.; Gallagher, R. C.; Karlsson, G.; Edwards, K.; Kenner, G.; Samuels, L.; Webb, M. S.; Bally, M. B. Influence of poly(ethylene glycol) grafting density and polymer length on liposomes: relating plasma circulation lifetimes to protein binding. *Biochim. Biophys. Acta* **2007**, *1768* (6), 1367−77.
(30) Price, M. E.; Cornelius, R. M.; Brash, J. L. Protein adsorption to polyethylene glycol modified liposomes from fibrinogen solution and from plasma. *Biochim. Biophys. Acta* **2001**, *1512* (2), 191−205.
(31) Champion, J. A.; Mitragotri, S. Role of target geometry in phagocytosis. *Proc. Natl. Acad. Sci. U.S.A.* **2006**, *103* (13), 4930−4.
(32) Geng, Y.; Dalhaimer, P.; Cai, S.; Tsai, R.; Tewari, M.; Minko, T.; Discher, D. E. Shape effects of filaments versus spherical particles in flow and drug delivery. *Nat. Nanotechnol.* **2007**, *2* (4), 249−55.
(33) Champion, J. A.; Walker, A.; Mitragotri, S. Role of particle size in phagocytosis of polymeric microspheres. *Pharm. Res.* **2008**, *25* (8), 1815−21.
(34) Champion, J. A.; Mitragotri, S. Shape induced inhibition of phagocytosis of polymer particles. *Pharm. Res.* **2009**, *26* (1), 244−9.
(35) Kamps, J. A.; Scherphof, G. L. Receptor versus non-receptor mediated clearance of liposomes. *Adv. Drug Delivery Rev.* **1998**, *32* (1−2), 81−97.
(36) Duncanson, W. J.; Figa, M. A.; Hallock, K.; Zalipsky, S.; Hamilton, J. A.; Wong, J. Y. Targeted binding of PLA microparticles with lipid-PEG-tethered ligands. *Biomaterials* **2007**, *28* (33), 4991−9.
(37) Komba, S.; Sasaki, S.; Machida, S. A new colorimetric test for detection of hydroxyl groups in solid-phase synthesis. *Terahedron Lett.* **207**, *48*, 2075−8.
(38) Litovsky, S.; Madjid, M.; Zarrabi, A.; Casscells, S. W.; Willerson, J. T.; Naghavi, M. Superparamagnetic iron oxide-based method for quantifying recruitment of monocytes to mouse atherosclerotic lesions in vivo: enhancement by tissue necrosis factor-alpha, interleukin-1beta, and interferon-gamma. *Circulation* **2003**, *107* (11), 1545−9.